Supplementary Information (SI) for Journal of Materials Chemistry A.
This journal is © The Royal Society of Chemistry 2024

Supplementary information

Polystyrene resin in suit supported PANI/Fe_3O_4 composite as heterogeneous Fenton catalyst for the efficient degradation of tetracycline in water

Jiaming Xu [a], Heng Zhang [a], Jinmao Ma [b], Lincheng Zhou [a, *],
Quanlin Zhao [b], Zhengfang Ye [b]

[a.] *State Key Laboratory of Applied Organic Chemistry, College of Chemistry and Chemical Engineering, Institute of Biochemical Engineering & Environmental Technology, Lanzhou University, Lanzhou 730000, PR China.*

[b.] *Department of Environmental Engineering, Peking University, the Key Laboratory of Water and Sediment Sciences, Ministry of Education, Beijing 100871, China*

* Corresponding author

E-mail address: zhoulc@lzu.edu.cn (L. Zhou).

Text S1 Reagents and Materials

Polystyrene resin (PS) was provided by Xi'an Jinwotai Environmental Protection Technology Co., Ltd. (Xi'an, China). Chloroform ($CHCl_3$), urea, concentrated nitric acid (68% HNO_3), concentrated sulfuric acid (98% H_2SO_4), concentrated hydrochloric acid (36% HCl), sodium hydroxide (NaOH), and stannous chloride ($SnCl_2$) were purchased from Sichuan Xilong Science Co., Ltd. (Chengdu, China). Ethanol, Ammonium Hydroxide (28% $NH_3 \cdot H_2O$), ferrous chloride tetrahydrate ($FeCl_2 \cdot 4H_2O$), hexahydrate ferric chloride ($FeCl_3 \cdot 6H_2O$), and tetracycline (TC) were supplied by Anhui Zesheng Technology Co., Ltd. (Anqing, China). Argon was purchased from Lanzhou Hongli Gas Co., Ltd. (Lanzhou, China). Deionized water was homemade for the laboratory.

Text S2 Synthesis of APS

First, weighed 6 g of polystyrene resin (PS) and soaked them in 50 mL chloroform to swell. Filtered by suction to remove the solvent, 0.27 g of urea was added (to eliminate by-products) and then transferred to a 100 mL four-necked flask. Slowly added 11 mL of mixed acid composed of 10.5 mL 60% concentrated nitric acid and 22.5 mL concentrated sulfuric acid cooled with ice water, and then started stirring. The remaining mixed acid was slowly dropped within 1h, and the reaction temperature was controlled below 50 °C. The reaction was refluxed and stirred at 65–70 °C for 3 h. After the reaction was completed, cooled to room temperature, carefully poured the reactants into ice water, filtered, rinsed with water to neutral, and dried to obtain golden nitrified PS (NPS) (Fig. S1).

4.05 g of NPS was placed in a 250 mL round-bottom flask with 48 g of tin dichloride, 54 mL of concentrated hydrochloric acid, and 60 mL of absolute ethanol; and then refluxed in a boiling water bath for 10 h. At the end of reflux, the supernatant was discarded by pouring and the resin was washed with excess 2 mol/L NaOH solution until no white precipitate precipitated. The resin was then washed with 2 mol/L HCl solution and finally washed to neutrality with deionized water. The khaki aminated PS (APS) was obtained by vacuum drying at 60 °C for 12 h.

Text S3 Tauc Plot method

Most of the valence band (VB) electrons and conduction band (CB) electrons of semiconductors are distributed near the forbidden band, so when the photon energy is close to the width of the bandgap, a large number of electrons can transition by absorbing photon energy, and the absorption coefficient increases with increased the number of photons.

For semiconductor materials, the relationship between optical band gap and absorption coefficient is as follows: [1]

$$(\alpha h\nu)^{1/n} = \lambda(h\nu - E_g)$$

where α is the absorption coefficient, $h\nu$ is the photon energy, h is the Planck constant, ν is the incident photon frequency, λ is the proportional constant, and E_g is the band gap width of semiconductor materials. The n value is related to the type of semiconductor material. When the semiconductor material is a direct band gap, the n value is 1/2; when the semiconductor material is an indirect band gap, the n value is 2.

Table S1 the mass of PANI/Fe_3O_4/APS compared to APS before and after the two loadings.

Samples	1	2	3
APS (g)	1.6526	2.0561	1.8453
PANI/Fe_3O_4/APS (g)	1.9750	2.4332	2.2020
Loading mass (g)	0.3224	0.3771	0.3567

Table S2 The contents of C, N, O, and Fe elements of APS, Fe_3O_4/APS, and PANI/Fe_3O_4/APS by EDS scanning at three different points.

Samples	Scan positions	C		O		N		Fe	
		wt%	at%	wt%	at%	wt%	at%	wt%	at%
APS	1	64.96	69.52	14.64	11.76	20.40	18.72	-	-
	2	64.66	69.16	13.74	11.03	21.60	19.81	-	-
	3	70.39	74.57	13.03	10.36	16.59	15.07	-	-
Fe_3O_4/APS	1	50.99	64.78	21.69	20.69	8.67	9.44	18.65	5.09
	2	17.33	31.57	33.8	46.23	2.60	4.06	46.28	18.14
	3	52.78	65.81	19.92	18.65	10.26	10.97	17.03	4.57
PANI/Fe_3O_4/APS	1	52.36	62.83	25.93	23.36	10.64	10.95	11.07	2.86
	2	49.3	61.43	25.86	24.19	9.65	10.31	15.19	4.07
	3	52.91	62.31	22.51	19.90	15.29	15.44	9.29	2.35

Table S3 The surface area, pore volume, and pore size of APS, Fe_3O_4/APS, and PANI/Fe_3O_4/APS.

Sample	BET surface area (m^2/g)	t-Plot micropore area (m^2/g)	t-Plot external surface area (m^2/g)	t-Plot micropore volume (cm^3/g)	BJH cumulative volume of pores (nm)		BJH average pore diameter (4V/A) (nm)	
					Adsorption	Desorption	Adsorption	Desorption
APS	328.10	66.65	261.45	0.01088	0.8443	0.8426	12.47	12.16
Fe_3O_4/APS	606.76	256.13	350.63	0.1214	0.9012	0.8921	8.47	8.40
PANI/Fe_3O_4/APS	376.79	145.43	231.37	0.06469	0.5903	0.6208	9.71	9.28

Table S4 The additional information for VSM analysis of APS, Fe_3O_4/APS, and PANI/Fe_3O_4/APS.

Samples	coercivity (H_c, Oe)	remanence (M_r, emu/g)	squareness (S)
APS	-0.527	-1.323E-5	0
Fe_3O_4/APS	2.104	0.073	0.004
PANI/Fe_3O_4/APS	2.703	0.052	0.011
Fe_3O_4 powder	3.883	0.382	0.007

Table S5 Comparison of the TC degradation conditions and the removal efficiency of heterogeneous Fenton catalysts reported in different papers.

Catalyst	Oxidant	Time (min)	Additional conditions	Catalyst dosage (g/L)	Initial Conc. (mg/L)	Rate constant k (min^{-1})	Efficiency (%)	Ref.
α-Fe_2O_3/g-C_3N_4 heterojunction	H_2O_2 (50 mM)	180	300 W xenon lamp	0.5	20	0.01647	96.4	[2]
15Fe/SCN	H_2O_2 (80 mM)	80	300 W xenon lamp (λ>420 nm)	0.5	20	0.02690	90.3	[3]
magnetic α-FeOOH/γ-Fe_2O_3 nanocomposite	H_2O_2 (10 mM)	60	300 W xenon lamp (λ>420 nm)	0.5	10	0.07700	92.0	[4]
BC/FeOOH	H_2O_2 (15 mM)	90	300 W xenon lamp	1.0	20	0.02630	92.0	[5]
$FeMo_3O_x$/g-C_3N_4	H_2O_2 (20 mM)	60	500 W xenon lamp (λ>420 nm)	1.33	25	0.05694	98.0	[6]
$LaFeO_3$/zeolite	H_2O_2 (10 mM)	150	300 W xenon lamp (λ>400 nm)	1.0	10	0.01030	76.4	[7]
$Au_{0.1}Ag_{0.9}$/TiO_2/CA	In situ generation	120	300 W xenon lamp (λ>400 nm)	2.0	5	0.01276	77.4	[8]
NCQDs/MIL-101(Fe)	In situ generation	250	500 W xenon lamp	0.5	10	0.02060	~100	[9]
$CuInS_2$/Bi_2MoO_6	In situ generation	120	300 W xenon lamp (λ>400 nm)	0.6	15	0.01500	84.7	[10]
$CuFeO_2$/BC	H_2O_2 (50 mM)	300	-	0.5	20	0.00613	89.1	[11]
PANI/Fe_3O_4/APS	H_2O_2 (25 mM)	120	300 W Mercury lamp	1.0	20	0.03068	98.7	This Work

Table S6 Hirshfeld charge distribution of TC and Fukui index of f^-, f^+, and f^0.

Atom	q(N) (e/Å)	q(N+1) (e/Å)	q(N-1) (e/Å)	f^-	f^+	f^0
1(C)	-0.0743	-0.1099	-0.0524	0.0219	0.0356	0.0287
2(C)	-0.0294	-0.1045	0.0099	0.0393	0.0751	0.0572
3(C)	-0.0586	-0.0868	-0.0359	0.0227	0.0282	0.0254
4(C)	0.0077	-0.0325	0.0103	0.0026	0.0402	0.0214
5(C)	-0.0389	-0.0590	-0.0288	0.0101	0.0201	0.0151
6(C)	0.0906	0.0552	0.1141	0.0236	0.0354	0.0295
7(C)	0.0874	0.0850	0.0878	0.0004	0.0024	0.0014
8(C)	-0.0309	-0.0334	-0.0166	0.0143	0.0025	0.0084
9(C)	-0.0719	-0.0844	0.0767	0.1486	0.0125	0.0805
10(C)	0.1319	0.0365	0.1482	0.0162	0.0954	0.0558
11(C)	-0.0532	-0.0560	-0.0366	0.0166	0.0028	0.0097
12(C)	-0.0221	-0.0253	-0.0210	0.0011	0.0033	0.0022
13(C)	0.0698	0.0623	0.0713	0.0014	0.0075	0.0045
14(C)	0.1042	0.0302	0.1832	0.0790	0.0740	0.0765
15(C)	0.0228	0.0245	0.0211	-0.0016	-0.0017	-0.0017
16(C)	0.1154	0.1168	0.1123	-0.0031	-0.0014	-0.0023
17(C)	-0.0800	-0.0833	-0.0774	0.0026	0.0033	0.0030
18(C)	0.1438	0.1452	0.1400	-0.0038	-0.0014	-0.0026
19(O)	-0.1770	-0.2005	-0.1521	0.0249	0.0235	0.0242
20(O)	-0.2414	-0.3426	-0.1866	0.0548	0.1012	0.0780
21(O)	-0.1734	-0.2339	-0.0585	0.1149	0.0605	0.0877
22(O)	-0.2298	-0.2548	-0.2019	0.0279	0.0249	0.0264
23(O)	-0.2261	-0.2439	-0.2045	0.0216	0.0178	0.0197
24(C)	0.1781	0.1746	0.1798	0.0017	0.0036	0.0026
25(N)	-0.1506	-0.1579	-0.1424	0.0082	0.0073	0.0077
26(N)	-0.0919	-0.0911	-0.0895	0.0024	-0.0008	0.0008
27(O)	-0.2125	-0.2248	-0.1960	0.0165	0.0124	0.0144
28(C)	-0.0913	-0.1005	-0.0850	0.0064	0.0092	0.0078
29(O)	-0.1568	-0.1648	-0.1457	0.0111	0.0080	0.0095
30(O)	-0.2582	-0.2709	-0.2458	0.0124	0.0128	0.0126
33(C)	-0.0414	-0.0434	-0.0376	0.0038	0.0020	0.0029
34(C)	-0.0452	-0.0501	-0.0396	0.0056	0.0048	0.0052

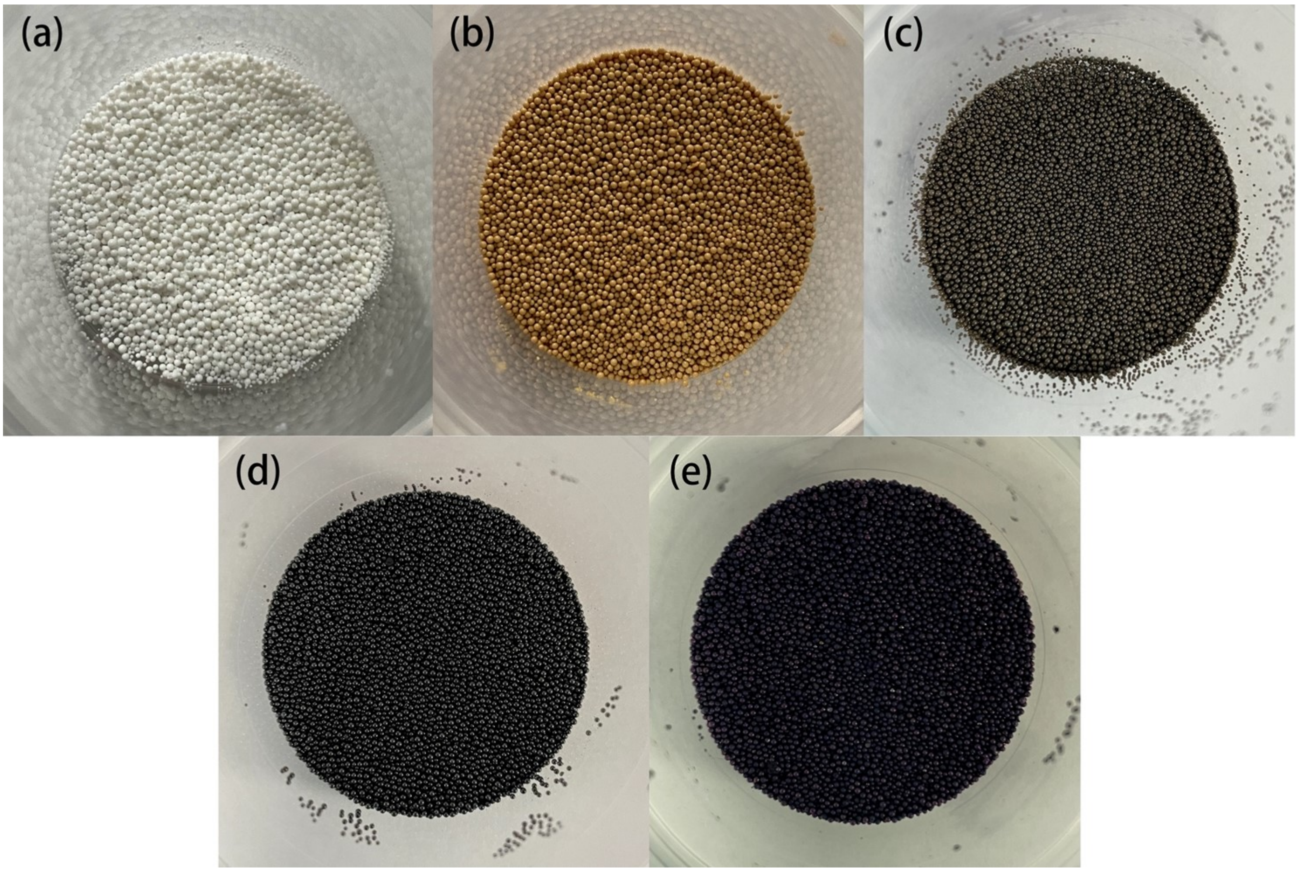

Fig. S1. The sample's pictures of (a) PS, (b) NPS, (c) APS, (d) Fe_3O_4/APS, and (e) PANI/Fe_3O_4/APS.

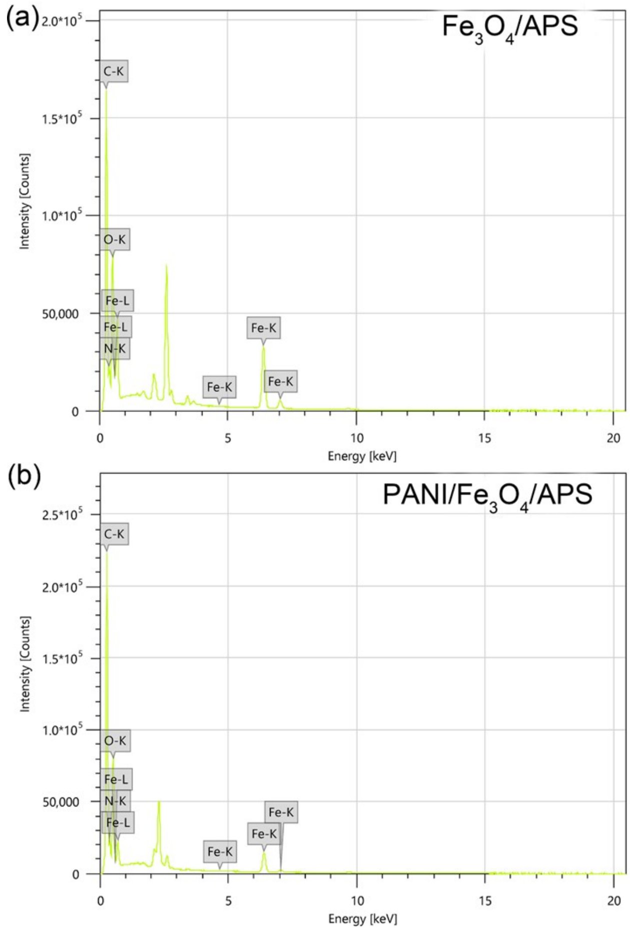

Fig. S2. EDS spectra of (a) Fe_3O_4/APS and (b) PANI/Fe_3O_4/APS.

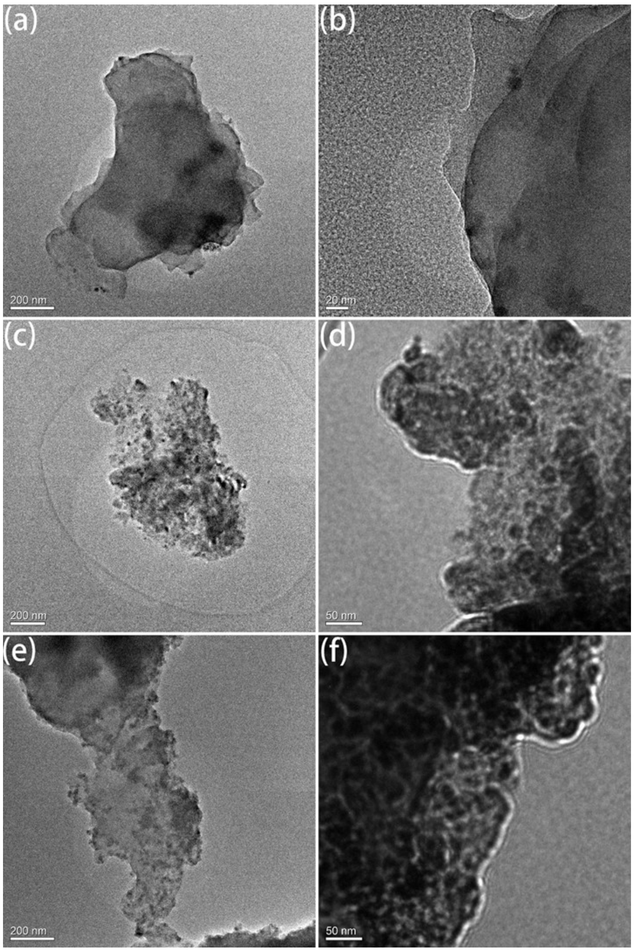

Fig. S3. TEM images of PANI/Fe_3O_4-X. (a, b) X=0.5, (c, d) X=1, and, (e, f) X=2.

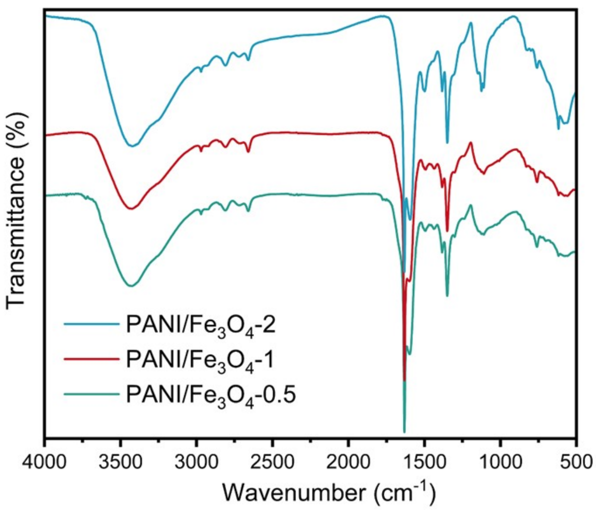

Fig. S4. FT-IR spectra of PANI/Fe_3O_4-X (X = 0.5, 1, and 2).

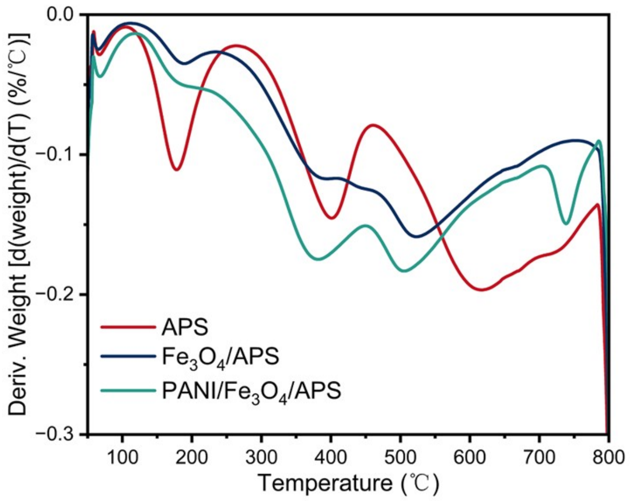

Fig. S5. DTG curves of APS, Fe_3O_4/APS, and PANI/Fe_3O_4/APS.

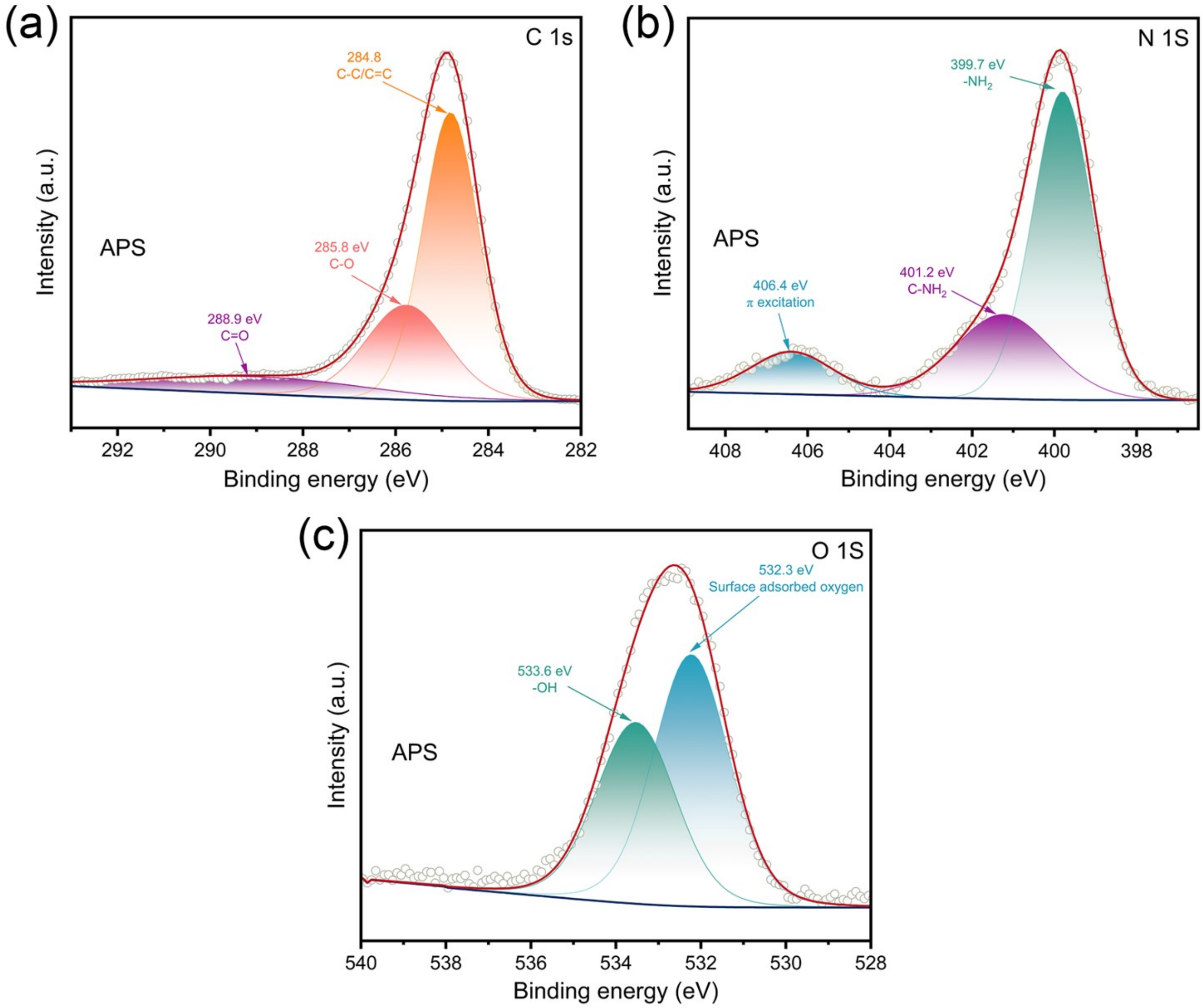

Fig. S6. High-resolution XPS spectra of (a) C 1s, (b) N 1s, and (c) O 1s of APS.

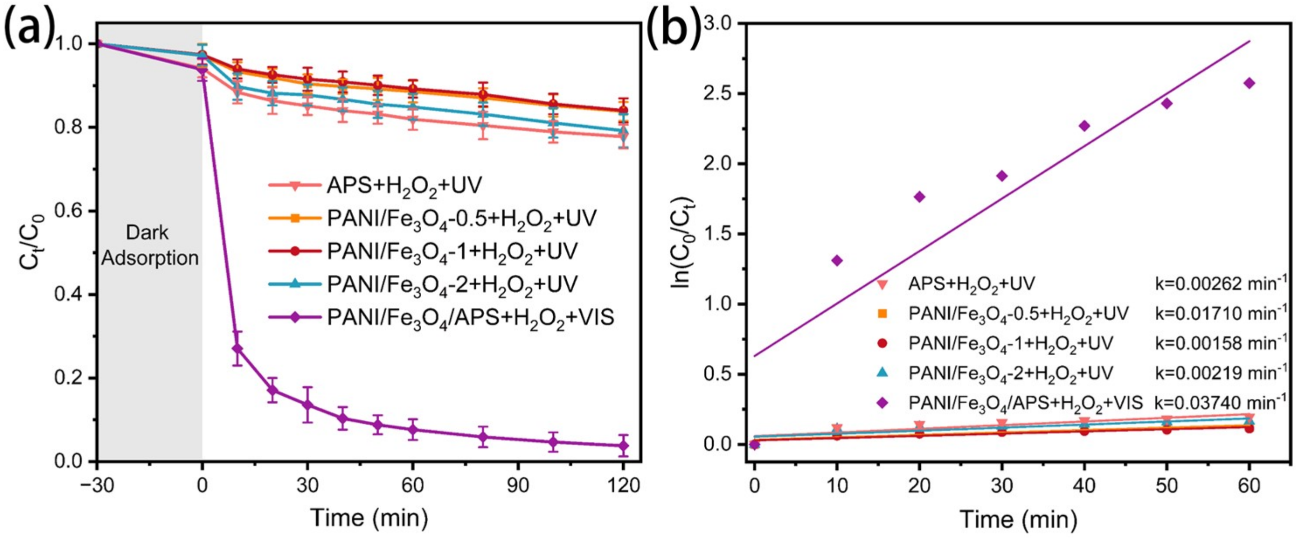

Fig. S7. (a) Removal of TC in different reaction systems and (b) corresponding pseudo-first-order kinetic curves. Experiment conditions: $[TC]_0$ = 20 mg/L, $[PANI/Fe_3O_4\text{-}X]$ = 0.16 g/L, $[PANI/Fe_3O_4/APS]$ = 1.0 g/L, [APS] = 1.0 g/L, $[H_2O_2]$ = 25 mM, pH = 6.95, T = 303 K.

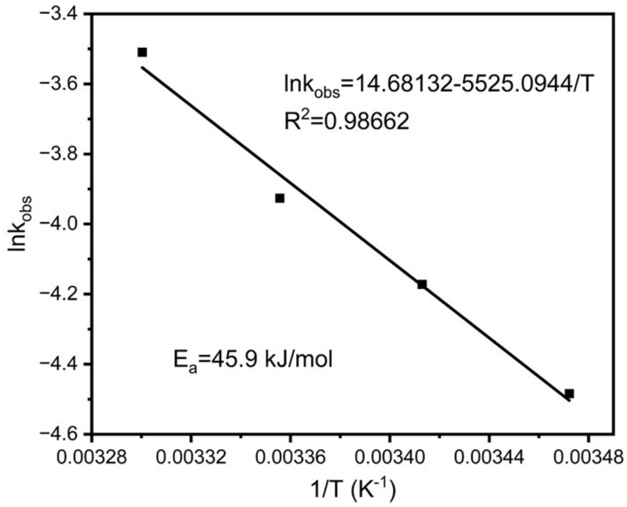

Fig. S8. Arrhenius curve at different temperatures.

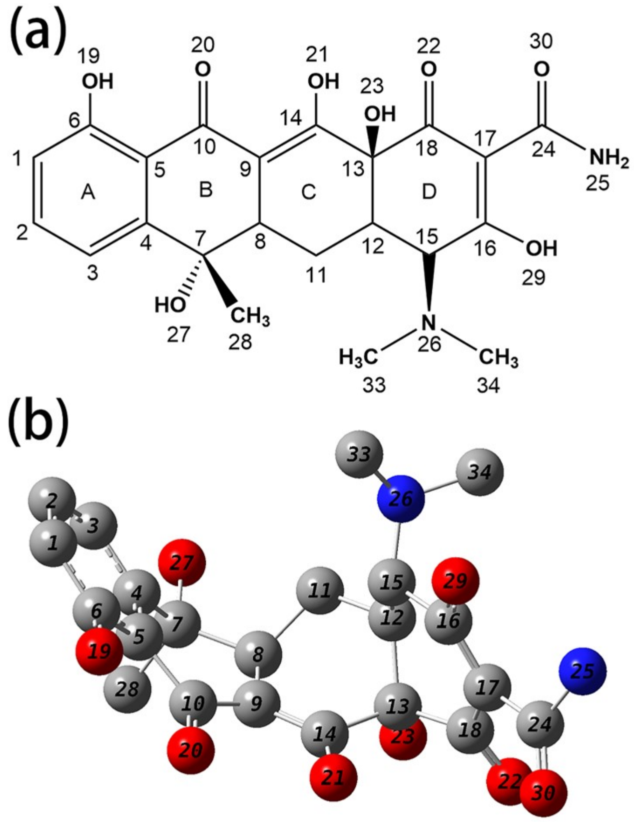

Fig. S9. The optimized structure and atomic number of TC. (a) skeletal formula and (b) ball-and-stick model.

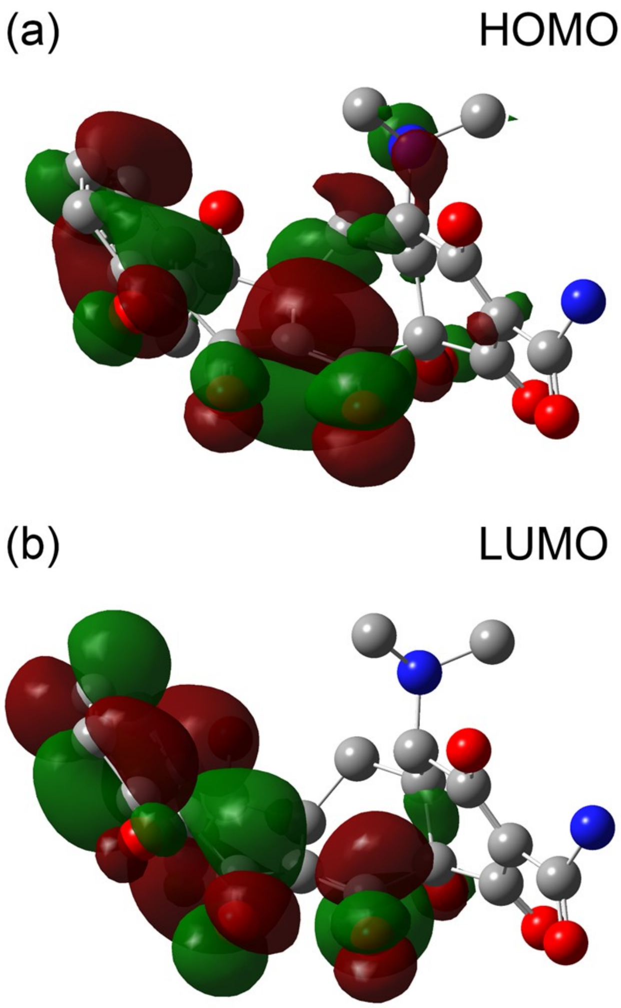

Fig. S10. (a) HOMO and (b) LUMO of the optimized structure of TC.

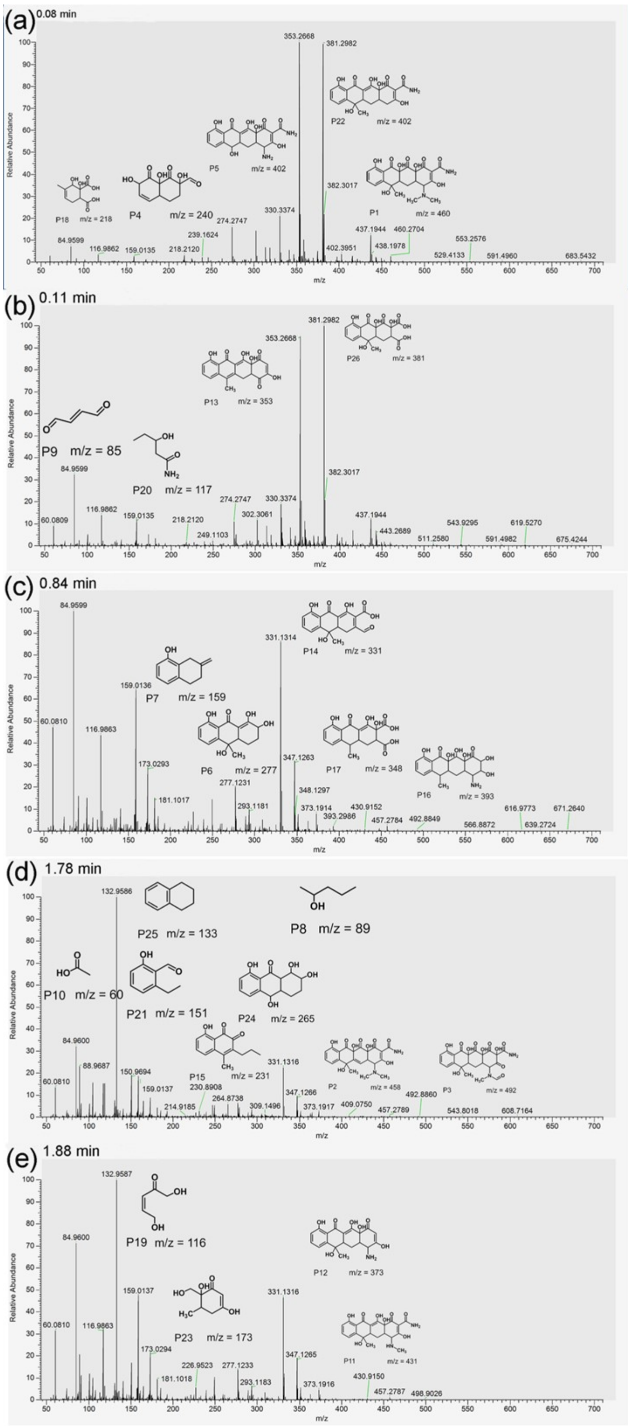

Fig. S11. HPLC-MS molecular mass profiles of the intermediates. Detection time: (a) 0.08 min; (b) 0.11 min; (c) 0.84 min; (d) 1.78 min; (e) 1.88 min.

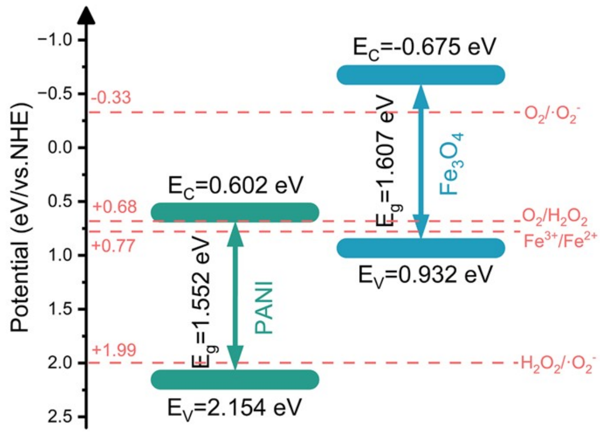

Fig. S12. Band gap structures of Fe_3O_4 and PANI.

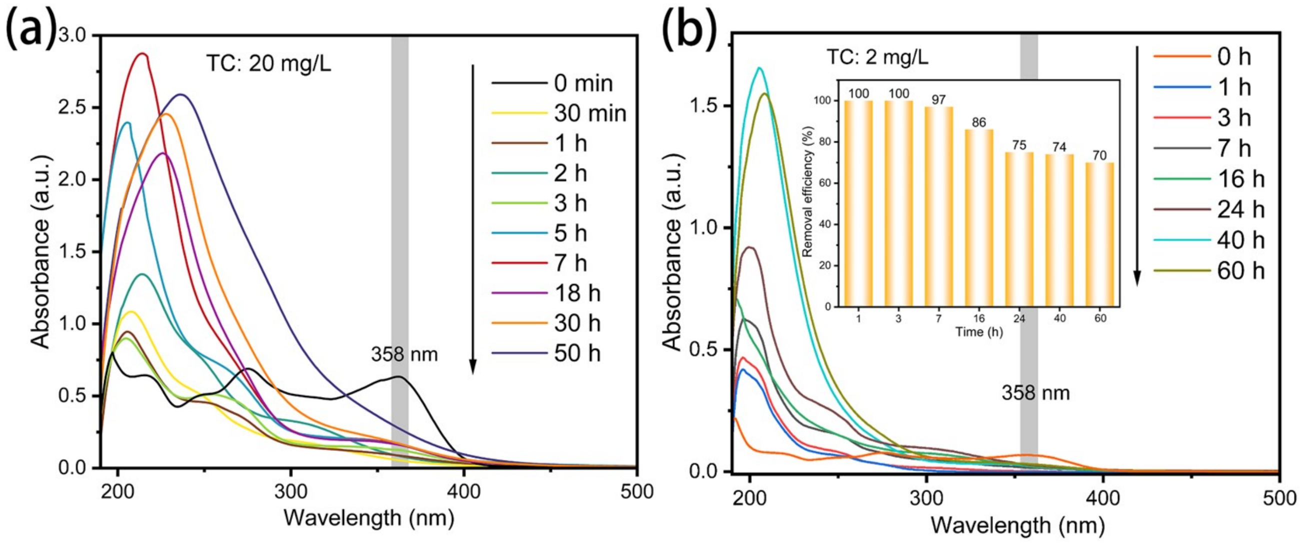

Fig. S13. UV-vis spectra contain absorbance at different times and wavelengths of catalytic device. TC concentration: (a) 20 mg/L and (b) 2 mg/L (inset is the corresponding removal efficiency of at different times). Reaction conditions: [PANI/Fe_3O_4/APS] = 3.0 g, [H_2O_2] = 25 mM, pH = 6.95, T = room temperature, current velocity = 1.0 mL/min.

Reference

1 A. Lin, M. Ren, X. Tan, J. Ma, Y. Zhang, T. Yang, Y. Pei and J. Cui, *J. Clean Prod.*, 2022, **345**, 131058.
2 F. Xu, B. Chai, Y. Liu, Y. Liu, G. Fan and G. Song, *Colloid Surf. A-Physicochem. Eng. Asp.*, 2022, **652**, 129854.
3 X. Li, X. Zhang, S. Wang, P. Yu, Y. Xu and Y. Sun, *J. Environ. Manage.*, 2022, **312**, 114856.
4 Y. Ma, B. Wang, Q. Wang and S. Xing, *Chem. Eng. J.*, 2018, **354**, 75–84.
5 Q. Xue, B. Song, Q. Feng, Z. Yu, K. Hu, Y. Yang and X. Shen, *Appl. Surf. Sci.*, 2024, **645**, 158869.
6 Y. Liu, X. Wang, Q. Sun, M. Yuan, Z. Sun, S. Xia and J. Zhao, *J. Hazard. Mater.*, 2022, **424**, 127387.
7 P. T. T. Nga, P. C. Nhan and T. T. T. Huyen, *Vietnam J. Chem.*, 2022, **60**, 76–83.
8 W. Li, B. Li, M. Meng, Y. Cui, Y. Wu, Y. Zhang, H. Dong and Y. Feng, *Appl. Surf. Sci.*, 2019, **487**, 1008–1017.
9 Y. Xie, C. Liu, D. Li and Y. Liu, *Appl. Surf. Sci.*, 2022, **592**, 153312.
10 J. Guo, L. Wang, X. Wei, Z. A. Alothman, M. D. Albaqami, V. Malgras, Y. Yamauchi, Y. Kang, M. Wang, W. Guan and X. Xu, *J. Hazard. Mater.*, 2021, **415**, 125591.
11 X. Shuaishuai, L. Guocheng, M. Xiaohan, G. Jiaxin, M. Bingrui, Y. Qinghua, C. Qinghua, M. Dong, Z. Guangshan, G. Mengchun and X. Yanjun, *Appl. Catal. B-Environ.*, 2021, **280**, 119386.